

Projectile structure effects in the collisions $^{6,7}\text{Li}+^{64}\text{Zn}$ around the Coulomb barrier

P.Figuera^{1a}, A.Di Pietro¹, M.Fisichella¹, M.Lattuada^{1,2}, C.Maiolino¹, M.Milin³, A.Musumarra^{1,2}, V.Ostashko⁴, M.G.Pellegriti¹, G.Randisi^{1,2}, D.Santonocito¹, V.Scuderi^{1,2}, E.Strano^{1,2}, D.Torresi^{1,2}, M.Zadro⁵

¹INFN Laboratori Nazionali del Sud, Catania, Italy

²Dipartimento di Fisica ed Astronomia Università di Catania, Catania Italy

³Department of Physics University of Zagreb, Zagreb, Croatia

⁴KINR, Kiev, Ukraine

⁵Ruder Boskovic Institut, Zagreb, Croatia

Abstract. We measured elastic scattering angular distributions and cross sections for heavy residue production for the systems $^{6,7}\text{Li}+^{64}\text{Zn}$ at different energies around the Coulomb barrier. The elastic scattering angular distributions have been reproduced by optical model fits using a renormalized double folding potential for the real and imaginary parts. Absence of usual threshold anomaly in the optical potential was found. The excitation functions for heavy residue production were measured using an activation technique. Comparison with different calculations suggest that complete fusion is the dominant reaction mechanism above the barrier whereas, below the Coulomb barrier, incomplete fusion and transfer dominate.

1 Introduction

The study of collisions induced by halo and weakly bound nuclei at energies near the Coulomb barrier had a considerable interest in the last decade since the peculiar structure of such nuclei can deeply affect the reaction mechanisms (See e.g. [1] and refs. therein). One expects in fact that, due to the halo or cluster structure with low binding energy, direct reaction mechanisms such as breakup and transfer become important. At the same time, effects of coupling to continuum are expected to be important both in elastic scattering (e.g. [2-9]) and fusion (e.g. [10,11]). As an example, the presence of a repulsive polarisation potential associated with continuum coupling may destroy the usual threshold anomaly in the Optical Potential (OP) (See e.g. [5-8]). The study of fusion reactions is complicated by the fact that one may have important incomplete fusion (ICF) contributions, following breakup of the projectile, competing with complete fusion (CF). Here we will discuss the results of some experiments, performed at the Catania Tandem, concerning the study of elastic scattering and Heavy Residue (HR) production in the collisions $^{6,7}\text{Li}+^{64}\text{Zn}$ at different energies near the Coulomb barrier.

^a Corresponding author: figuera@lns.infn.it

2 Elastic scattering

Elastic scattering angular distributions were measured at different energies using an array of 5 DE-E Si telescopes mounted on a rotating arm. The angular distributions, measured in a wide angular range ($10^\circ < \theta_{c.m.} < 170^\circ$), were reproduced by optical model fits, using renormalized double folding potentials for the real and imaginary parts as discussed in [8]. The renormalisation coefficients were left as free parameters in the fits; as an example, their obtained trend as function of energy for the system ${}^6\text{Li}+{}^{64}\text{Zn}$ is shown in figure 1(b). Absence of usual threshold anomaly was found for both collisions.

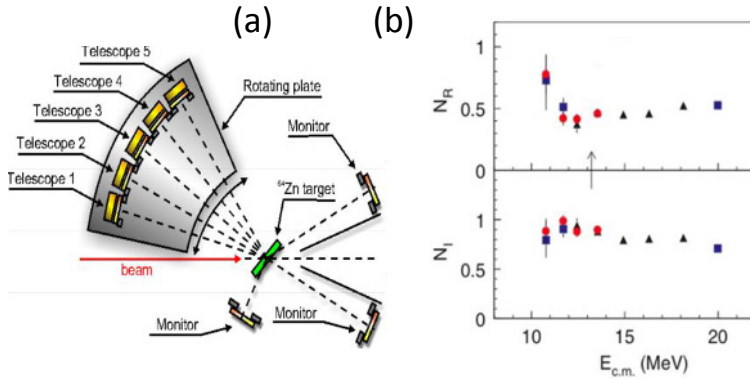


Figure 1. (Color online) (a) Sketch of the experimental setup used for the elastic scattering measurement. (b) Energy dependence of the renormalisation coefficients for the real and imaginary part in ${}^6\text{Li}+{}^{64}\text{Zn}$, showing clear absence of the usual threshold anomaly; the different symbols correspond to the results of independent measurements. The arrow indicates the position of the Coulomb barrier

3 Heavy residue excitation functions

The cross sections for heavy residue production have been measured by using an activation technique, detecting off line the atomic X rays emitted after the electron capture decay of the residues. This technique allows to avoid the energy threshold problems typical of the direct detection of the HR,

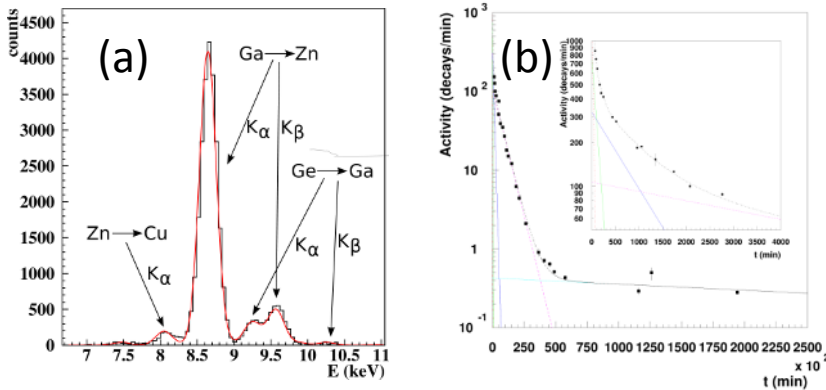


Figure 2. (Color online) (a) Off line X-ray energy spectrum for the collision ${}^6\text{Li}+{}^{64}\text{Zn}$ at $E_{\text{LAB}}=20$ MeV, measured about 7 hours after the end of the activation. $K\alpha$ and $K\beta$ lines corresponding to the decay of Zn, Ga and Ge isotopes are clearly visible. (b) Activity curve for the Ga $K\alpha$ peak for the collision ${}^7\text{Li}+{}^{64}\text{Zn}$ at $E_{c.m.}=28.3$ MeV. Different slopes corresponding to known half-lives of the produced Ga isotopes are clearly visible. (See text for details).

allowing to measure the production cross sections at energies below the Coulomb barrier. ^{64}Zn targets, followed by Nb and Ho catchers capable of stopping all produced heavy residues, have been irradiated by $^{6,7}\text{Li}$ beams. The beam current during irradiation was measured via Rutherford scattering on a thin Au foil. After irradiation, the targets were placed in front of lead shielded Si-Li detectors in order to look for the atomic X rays following the HR electron capture decay. A typical X ray spectrum measured for the collision $^6\text{Li}+^{64}\text{Zn}$ at 20 MeV is shown in figure 2(a). As one can see, a clear identification of the $K\alpha$ peaks corresponding to different elements allows charge identification of the produced HR. Moreover, following the activity of each peak as a function of time, since isotopes of a given element have different half lives, the contribution of different isotopes for a given atomic number has been obtained. As an example, in figure 2(b) we show the activity of the Ga peak for the reaction $^7\text{Li}+^{64}\text{Zn}$ at $E_{c.m.}=28.3$ MeV. The production cross sections of the various isotopes have been obtained, as in [12,13], analysing these activity curves and taking into account different factors such as: beam current as function of time during activation, $K\alpha$ fluorescence probability, X-ray detection efficiency and X-ray absorption in the catcher and target foils. Excitation functions for HR production are shown in figure 3, together with the results of single barrier penetration (SBP) and coupled channels (CC) calculations including the excitation of different states of projectile and target. As one can see, both calculations reproduce the data above barrier but fail below it. In order to understand which are the possible reaction mechanism responsible for heavy residue production, the experimental relative yield of the HR was compared with different statistical model calculations performed using the code Cascade [15].

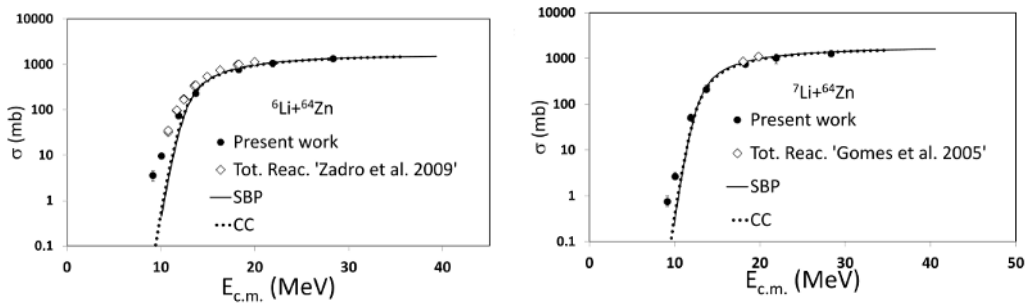


Figure 3. Excitation functions for heavy residue production (full circles) and total reaction (open diamonds) for the systems $^6\text{Li}+^{64}\text{Zn}$ and $^7\text{Li}+^{64}\text{Zn}$. The total reaction data are from refs [8, 14].

Since ^6Li and ^7Li have weakly bound cluster structures of the ground state with separation energies $S_\alpha=1.47$ and $S_\alpha=2.47$ MeV respectively, we expect reactions where only an alpha particle, a deuteron or a tritium are captured by the target. This may happen in two different ways, breakup followed by incomplete fusion (ICF) or a direct cluster transfer (DCT). Since ICF and DCT populate the same nuclei with similar excitation energies, we cannot distinguish between the two modes in the present experiments. Expected relative yields of the HR populated in ICF or DCT have been calculated with Cascade. The excitation energies following the d, t or α capture were estimated assuming an ICF mechanism where the available fragment-target centre of mass energy before ICF occurs is: $(E_{c.m.} - S_\alpha) \times (m_{clu} / m_{proj})$. Here $E_{c.m.}$ is the initial centre of mass energy of the $\text{Li}+^{64}\text{Zn}$ system, S_α is the α separation energy of the projectile and m_{clu} and m_{proj} are the masses of the captured cluster and of the projectile respectively. Excitation energies estimated for DCT were only slightly smaller than the ones for ICF, giving basically the same relative yield as for ICF. A comparison between the experimental HR relative yield and the Cascade calculations shows that above barrier the experimental relative yields are similar to the ones predicted by CF Cascade calculations, showing that CF is the dominating mechanism. However, at energies below the barrier, the HR experimental relative yield is rather different than the one expected for CF, showing that CF is no longer the dominating reaction mechanisms while other processes such as ICF, DCT or single nucleon transfer

become very important. As an example, in figure 4 we compare the HR experimental relative yield with the prediction of Cascade statistical model calculations for CF and ICF/DCT at $E_{c.m.}=10.1$ MeV ($V_{Coul.} \sim 13$ MeV [8]). As one can see, for ${}^6\text{Li}+{}^{64}\text{Zn}$ the relative yield is dominated by ${}^{65}\text{Zn}$ and ${}^{65}\text{Ga}$ which are not expected in CF but can be produced in ICF/DCT of a deuteron as well as in 1n and 1p transfer reactions respectively. For ${}^7\text{Li}+{}^{64}\text{Zn}$ the experimental yield is dominated by ${}^{65}\text{Zn}$ and ${}^{66}\text{Ga}$ whose yield is not expected to be important in CF but can be explained as due to 1n transfer and tritium ICF/DCT.

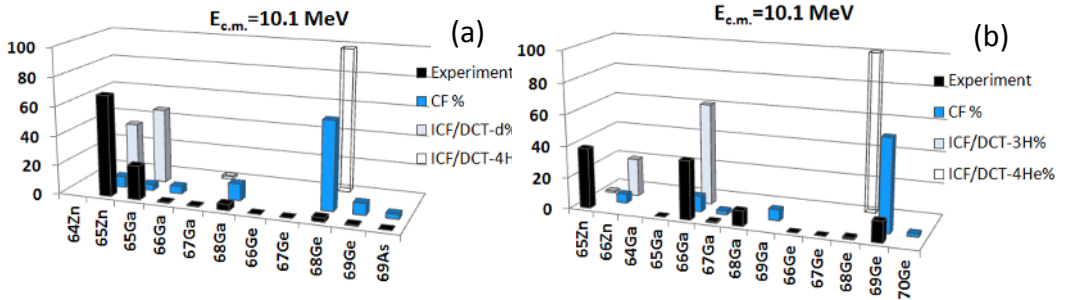


Figure 4. (Color online) Experimental heavy residue relative yield for ${}^6\text{Li}+{}^{64}\text{Zn}$ (a) and ${}^7\text{Li}+{}^{64}\text{Zn}$ (b) at $E_{c.m.}=10.1$ MeV, compared with the prediction of statistical model calculations for complete fusion and deuteron, tritium or α capture. See text for details.

In summary, the present results suggest that new experiments capable of distinguishing the contribution of different reaction mechanisms are necessary for a deeper understanding of fusion in collisions induced by weakly bound projectiles because the simple integration of the heavy residue yield leads to a cross sections which can be different from the ones for CF and for CF+ICF.

References

1. L.F. Canto et al., Phys. Rep. **424**, 1 (2006)
2. M. Cubero et al., Phys. Rev. Lett. **109**, 262701 (2012)
3. A. Di Pietro et al., Phys. Rev. Lett. **105**, 022701 (2010)
4. A. Di Pietro et al., Phys. Rev. C **85**, 054607 (2012)
5. H.Kumawat et al., Phys. Rev. C **78**, 044617 (2008)
6. J.M. Figueira et al., Phys. Rev. C **81**, 024613 (2010)
7. A.M.M. Maciel et al., Phys. Rev. C **59**, 2103 (1999)
8. M. Zadro et al., Phys. Rev. C **80**, 064610 (2009)
9. M. Zadro et al., Phys. Rev. C **87**, 054606 (2013)
10. L. F. Canto et al., Nucl. Phys., A **821**, 51 (2009)
11. P.R.S. Gomes et al., Phys. Rev. C **79**, 027606 (2009)
12. A. Di Pietro et al, Phys. Rev. C **69**, 044613 (2004)
13. V.Scuderi et al., Phys. Rev. C **84**, 064604 (2011)
14. P.R.S. Gomes et. al., Phys. Rev. C **71**, 034608 (2005)
15. F.Puhlhofer, Nucl. Phys. A **280**, 267 (1977)